Thermo-physical behaviour and dynamic thermal properties of crumb rubber-modified concrete for energy efficiency in buildings

Khalid B Najim [a]* and Matthew R Hall [a]

[a] Nottingham Centre for Geomechanics, Division of Materials, Mechanics and Structures, Faculty of Engineering, University of Nottingham, University Park, Nottingham NG7 2RD, UK, Tel: +44 (0) 115 846 7873, Fax: +44 (0) 115 951 3159,

*corresponding author's E-mail: laxkbn@nottingham.ac.uk

Abstract

Experimental data is presented for the dry- and saturated steady state thermo-physical properties, and also the dynamic thermal properties, of 180, 120 and 65mm target slump mix designs for Plain Rubberised Concrete (PRC) with varying %wt rubber substitution and aggregate replacement types (fine, coarse, and mixed). The composites had significantly lower density and thermal conductivity than plain concrete, and there was an inverse relationship between thermal admittance and a) mix design target slump, and b) %wt crumb rubber substitution. The thermal decrement remained almost constant, and yet the associated time lag can be increased significantly.

Keywords: thermo-physical properties; rubberised concrete; energy efficiency

Nomenclature

c_{dry}	dry state specific heat capacity	J/(kg·K)
c_{sat}	saturated state specific heat capacity	J/(kg·K)
f	decrement factor	-
F	surface factor	-
$\bar{T}$	mean temperature	ºC
HFM	heat flow meter output	mV
q_{is}	internal surface heat flux	W/m^2
q_{es}	external surface heat flux	W/m^2
n_{ap}	apparent porosity	%
T_{ei}	internal environmental temperature	°C
T_{eo}	external environmental temperature	°C
U	Thermal transmittance	W/(m^2·K)
Y	Thermal admittance	W/(m^2·K)
κ	surface heat capacity (100mm depth)	kJ/(m^2·K)
κ_{30}	surface heat capacity (30mm depth)	kJ/(m^2·K)
λ_{dry}	dry state thermal conductivity	W/(m·K)
λ_{sat}	saturated state thermal conductivity	W/(m·K)
ρ_{dry}	dry density	kg/m^3
ρ_{sat}	saturated density	kg/m^3
ϕ	thermal admittance time lag	hr
ψ	surface factor time lag	hr
ω	decrement factor time lag	hr

1. Introduction

The continued growth in world population and the development in living standards have led to considerable increases in global energy consumption and this coupled with global warming phenomena effects (Najim and Hall 2011B). To rationalise mean annual operational energy consumption in residential buildings, which consumed more than 30% of total global energy consumption(Dong et al., 2004), thermally efficient building materials is highly recommended to be used (Al-Hadhrami et al., 2009). The design of optimum building fabric performance therefore requires a trade-off between dynamic thermal behaviour (temperature buffering and thermal storage) and thermal resistance to heat transfer, where a combination of minimal thermal storage but high thermal resistance is required (Dong et al., 2004).

Concrete, (in block, monolithic and Insulate Concrete Formwork (ICF) configurations) is one of the mostly widely used materials for load bearing external walls and/or internal partitions where high ‘thermal mass’ is required for incorporation into the wall fabric design. Aggregate physical properties are one of the most influential factors affecting concrete thermal insulation (Alexander and Mindess, 2005), thus using low thermal conductivity aggregates coupled with increased air entrainment is a logical way to improve concrete thermal resistance(Khan, 2002). Plain Rubberised Concrete (PRC) is an ordinary strength (low-high slump) class of concrete with coarse and/or fine rubber aggregate (chipped, crumb or fibre) replacement. PRC typically has good properties in terms of thermal and acoustic resistance, kinetic/vibrational energy absorption, impact resistance, and dynamic mechanical properties, a detailed review

of research relating to these materials was recently produced by (Najim and Hall, 2010). An added advantage to PRC is that the vast accumulation of end-of-life vehicle tyres presents serious environmental problems (Ganjian et al., 2009) leading to an EU ban on stockpiling since 2006(Paine and Daher, 2010) and efforts being made to utilise them in beneficial manner, e.g. as alternative aggregates that avoids landfill and primary aggregates levy taxation.

The vast majority of research studies have evaluated the mechanical and fresh properties of PRC materials, and only a limited number of handful studies have examined their thermal properties (Najim and Hall, 2010). Concrete thermal conductivity is mainly dependent on the pore moisture content and aggregate volume fraction, and (to a lesser degree) also on age, water/cement ratio, and admixture type(s) (Kim et al., 2003) in addition to the measuring equipment itself (Neville, 1995).

The aim of this study was to experimentally characterise the thermo-physical properties of PRC concrete materials by investigating the influence of basic mix design (target slump), %wt crumb rubber replacement, and aggregate replacement type, i.e. coarse replacement (CR), fine replacement (FR), and 50:50 fine and coarse replacement (CFR). These basic properties could then be used to determine and evaluate the dynamic thermal characteristics of PRC wall elements in terms of thermal storage and temperature buffering. It is important to highlight that all the data presented in this work have previously been published elsewhere (Najim and Hall, 2011)

2. Materials specification and mix design

A previous study by the authors (Najim and Hall, 2011A) has shown that structural concrete (f_c' > 17MPa, ρ_d = $\geq$ 2000 kg/m^3) can be designed with aggregate substitution by crumb rubber up to 20%wt FR, or up ~15%wt CR and CFR replacement types. Potentially, up to 30%wt of all replacement types could be used for non-structural applications e.g. lightweight block partitions. This research has also shown that the addition of crumb rubber aggregate has a significant effect on concrete mix air entrapment, and as a result provides a reduced slump whilst maintaining a high compaction factor in the plastic state. However, the effects of this on dynamic thermal properties and behaviour have not been studied previously.

For the materials used in this study, high strength (52.5 MPa) CEM I class Portland cement was used, with 10mm quartzite natural gravel (G = 2.60, A = 1.2), and 5mm down natural grit sand (G = 2.65, A = 1.1%), both sourced from Hope Valley, UK. In addition, 2-6 mm regular crumb rubber particles sourced from J Allcock & Sons, Manchester, UK. Three types of PRC mix designs were tested based on three different target slump values; high (180mm), medium (120mm), and low (65mm). For each slump level the %wt crumb rubber aggregate replacement was varied between 10%wt, 20%wt, and 30%wt for FR, CR, and CFR, plus a control mix with 0% replacement, giving a total of thirty mixes. For this study, specimens were prepared as 300 x 300mm slabs with a thickness of 50mm, based on ASTM C 192-88 (ASTMC192/C192M, 2007), and covered by a polyethylene sheet until final setting had occurred (24 hours ±2), after which the samples were de-moulded, labelled and submersed in a temperature-controlled water curing tank at 20ºC ±2 for 28 days. The particle-size distribution and specific surface area for the fine aggregate (FA), coarse

aggregate (CA), and crumb rubber aggregate are presented in a previous study(Najim and Hall, 2011A) along with experimental data for compaction factor, compressive strength (f_c'), and indirect tensile (splitting) strength, dynamic Modulus of Elasticity (E_d), and Ultrasonic Pulse Velocity (UPV). In addition to this, the chemical composition and physical properties of the crumb rubber are also provided.

3. Characterisation of thermo-physical properties

The specific heat capacity, c_p of each mix design was calculated as the sum of constituent heat capacities and weighted by their %wt proportions. The experimental values for the natural aggregate, crumb rubber, and Hardened Cement Paste (HCP) were presented in a previous study (Najim and Hall 2011B), where the mean value of five readings was taken across the range -13 ˚C to 57 ˚C and determined using a Differential Scanning Calorimeter (Q10 DSC, TA Instruments). In the dry state, air within open voids was assumed to have negligible heat capacity since it has a density of ~1.205 kg/m^3 at ambient temperatures and is assumed to have zero mass for the purposes of gravimetric material bulk density calculations. The specific heat capacity of concrete in both the dry (c_p) and moisture-dependent state (c_p^*) are calculated from Equations 1 and 2, respectively (Keikha et al., 2011).

$$\boldsymbol{c_p = \frac{1}{w_{total}}\left[m_{HCP}c_{HCP} + m_{CA}c_{CA} + m_{FA}c_{FA} + m_{CR}c_{CR}\right]} \qquad \text{Eq.1}$$

$$\boldsymbol{c_p^* = c_p + \frac{n_{ap}\cdot\rho_{water}}{m_{total}}\cdot c_{water}} \qquad \text{Eq. 2}$$

The dry and saturated state specific heat capacities for each of the thirty (reference and PRC) mixes used for this study are given in Tables 1, 2 and 3, corresponding to slump values of 180, 120 and 65, respectively. The thermal conductivity of concrete specimens, following immersion in water (λ^*) and oven-dried (λ) conditions, were experimentally determined using a computer-controlled P.A. Hilton B480 uni-axial heat flow meter apparatus with downward vertical heat flow, which complies with ISO 8301: 2010 (ISO8301:1991/Amd1:2010, 2010). Two slabs with dimensions of 300 ×300mm, and a typical thickness of 50mm, were prepared for each mix design and the mean average of two readings were obtained per slab specimen in both oven-dried and saturated states. For thermal conductivity measurement in saturated state, the concrete slabs were removed from the water curing tank at the end of their 28-day curing period and sealed in a vapour-tight envelop to prevent any change in moisture content. The influence of the thin envelop on the thermal conductivity of the slab specimens was found to be negligible when measuring thermal conductivity at a steady state variance of 2 - 3%, as prescribed by ISO 8301: 2010. In the dry state, all specimens were oven dried at 105±5˚C until the variation in mass was less than 0.2 % over a 24 hr period, before cooling to ambient laboratory temperature in a desiccator prior to testing. The thermal conductivity is calculated from the apparatus output using the following equation (Hall and Allinson, 2009):

$$\lambda = \frac{(d * \left[\left(k1 + (k2 * \bar{T}) + \left(\left(k3 + (k4 * \bar{T})\right) * HFM\right) + \left(\left(K5 + (k6 * \bar{T})\right) * HFM\right)\right]\right)}{dT} \quad \text{Eq. 3}$$

Calibration constants (*k*1 – *k*6) are determined prior to testing using standard reference specimens of know thermal conductivity determined by an absolute method. The thermo-physical characteristics of PRC materials are quite unusual since the effect of crumb rubber replacement appears to be a reduction in thermal conductivity but an increase in heat capacity. The reduction in conductivity can be attributed partly to the air entrapment effect of non-wetting rubber particles, resulting in significantly increased apparent porosity, but also to the lower thermal conductivity of crumb rubber particles themselves. In higher rubber replacement mixes the relative increase in saturated-state thermal conductivity compared with dry-state is due to the increased apparent porosity giving greater natural convection heat flow within the pore network when filled with water. Despite the associated reductions in bulk density with rubber replacement, the higher specific heat capacity of rubber particles gives an overall increase in heat capacity for the PRC materials (see Tables 1 – 3). The implications of these results are that PRC materials could be useful for building fabric to reduce thermal transmittance whilst enhancing thermal buffering.

4. Dynamic thermal admittance properties

These were determined for a 100mm thick solid concrete exposed external wall, based on ISO 13790: 2004 (ISO13790:2004, 2004), and the 'Dynamic Thermal Properties Calculator' software tool from the concrete centre 2010. The calculations assumed a vertical wall with horizontal heat flow and conventional surface boundary layer heat transfer coefficients of R_{si} = 0.13 m^2 K/W, and R_{so} = 0.04 m^2 K/W, taken from ISO 6946: 2007 (ISO6946:2007, 2007). The values for all %wt crumb rubber replacement amounts and aggregate types, for 180mm, 120mm and 65mm slump PRC mix designs, are given in Tables 4, 5 and 6, respectively. The *Y*-value of all

three reference mixes is very similar, and the effect of crumb rubber replacement appears to reduce *Y* whilst increasing associated lead time. This suggests that the use of PRC materials for exposed internal fabric may have a slightly lower heat flux from the internal environmental node and at a slower rate. Therefore, in climates where the cooling season dominates annual mean operational energy use, the reduction in the annual load as a result of passive cooling could be slightly lower assuming surface area and wall thickness are constant.

Another interesting effect of rubber replacement is that thermal decrement remains almost constant in all cases, whilst the associated time lag increases but the *U*-value decreases. This suggests that for heat exchange between the internal environmental node and the sol-air node (in either direction), higher rubber content in PRC walls reduces the total heat flux and the rate of change in heat flux as a result of internal/external temperature fluctuation, i.e. a higher thermal buffering effect. This dynamic thermal response is illustrated by the graphs shown in Figures 1, 2 and 3, representing each of the three mix classes. There appears to be no significant difference in internal environmental node temperature fluctuation. However, an increase in %wt rubber replacement appears to cause a significant and proportional reduction in internal surface heat flow, peaking at almost a 1 W/m^2 K reduction at 30% CR or CFR replacement in all three slump classes. This behaviour appears to be due to the fact that rubber aggregate substitution produces PRC materials with increased thermal resistance but also increases volumetric heat capacity, in comparison with plain concrete materials.

5. Conclusion

The substitution of crumb rubber for mineral aggregate in concrete appears to cause a significant reduction in thermal conductivity. As the %wt addition of crumb rubber increases, there is a greater moisture-dependent effect on the saturated-state thermal conductivity due to the increased apparent porosity caused by air entrapment. There appears to be an inverse relationship between the thermal admittance of concrete and both a) the mix design target slump value, and b) the %wt crumb rubber substitution. Whilst the volumetric heat capacity of concrete increases with %wt rubber addition, thermal admittance decreases and hence a PRC wall can store more heat energy but offers greater resistance to exchange of that heat with the surrounding environment. A further interesting effect of the rubber is that thermal decrement remains almost constant regardless of the %wt rubber addition, and yet the associated time lag increases significantly. Further research is required to better understand how the unique thermo-physical behaviour of PRC materials can be better exploited.

Acknowledgements

The authors wish to acknowledge the support of the Iraqi Government for Khalid Najim's research scholarship, which enabled this work to be conducted as part of a larger research project.

6. References

AL-HADHRAMI, M., L. & AHMAD, A. 2009. Assessment of thermal performance of different types of masonry bricks used in Saudi Arabia. *Applied Thermal Engineering,* 29**,** 1123-1130.

ALEXANDER, M. & MINDESS, S. 2005. *Aggregate in concrete,* London and New Yourk, Taylor & Francis Group.

ASTMC192/C192M 2007. Standard Practice for Making and Curing Concrete Test Specimens in the Laboratory.

DONG, Z., ZONGJIN, L., JIANMIN, Z. & WERU, K. 2004. Development of thermal energy storage concrete *Cement and Concrete Research,* 34**,** 927-934.

GANJIAN, E., KHORAMI, M. & MAGHSOUDI, A. A. 2009. Scrap-tyre-rubber replacement for aggregate and filler in concrete. *Construction and Building Materials,* 23**,** 1828-1836.

HALL, M. & ALLINSON, D. 2009. Assessing the effects of soil grading on the moisture content-dependent thermal conductivity of stabilised rammed earth materials. *Applied Thermal Engineering,* 29**,** 740-747.

ISO6946:2007 2007. Building components and elements: Thermal resistance and thermal trasmittance-calculation method. *International Organisation for standaraisation*.

ISO8301:1991/AMD1:2010 2010. Thermal insulation: Determination of steady-state thermal resistance and related properties-heat flow meter apparatus. *International Organisation for standaraisation*.

ISO13790:2004 2004. Thermal performance of building-calculation of energy use for space heating *International Organisation for standaraisation*.
KEIKHA, P., HALL , M. & DAWSON, A. 2011. Thermo-Physical Optimisation of Specialised Concrete Pavement Materials for Surface Heat Energy Collection and Shallow Heat Storage Applications. *Transportation Research Board 2011 Annual Meeting.* Washington DC, USA.
KHAN, M. I. 2002. Factors affecting the thermal properties of concrete and applicability of its prediction models. *Building and Environment,* 37**,** 607-614.
KIM, K.-H., JEON, S.-E., KIM, J.-K. & YANG, S. 2003. An experimental study on thermal conductivity of concrete. *Cement and Concrete Research,* 33**,** 363-371.
NAJIM, K. & HALL, M. 2011A. The influence of workability and air entrainment on the physico-mechanical properties of crumb rubber-modified concrete composites. *Submitted to Proceedings of the Institution of Civil Engineers ICE, construction Materials Journal*
NAJIM, K. & HALL , M. 2011B. Thermo-physical and mechanical analysis of Self-Compacting Rubberised Concrete (SCRC) mix classes. *Proceedings of the 13th International Conference on Non-conventional Materials and Technologies (13 NOCMAT 2011) 22nd – 24th September, Changsha, Hunan, China.*
NAJIM, K. B. & HALL, M. R. 2010. A review of the fresh/hardened properties and applications for plain (PRC) and self-compacting rubberised concrete (SCRC). *Construction and Building Materials,* 24**,** 2043-2051.
NEVILLE, A. M. 1995. *Properties of Concrete,* London, Longman.
PAINE, K. & DAHER, R. K. 2010. Research on new applications for granulated rubber in concrete *Proceedings Institution of Civil Engineers* 163**,** 7-17.

Table 1: Dry and saturated thermo-physical properties for 180mm slump PRC mixes

	ρ_d	ρ_{sat}	n_{ap}	λ_{dry}	λ_{sat}	c_{dry}	c_{sat}
	kg/m^3	kg/m^3	%	W/(m K)	W/(m K)	J/(kg K)	J/(kg K)
Ref.	2288	2372	3.5	1.172	1.315	907	970
FR 10%	2113	2227	5.1	1.089	1.268	927	1019
FR20%	2056	2179	5.6	1.001	1.172	948	1049
FR30%	1913	2044	6.4	0.844	1.050	968	1083
CR10%	2063	2188	5.7	1.068	1.249	938	1040
CR20%	1905	2038	6.5	0.953	1.084	968	1084
CR30%	1772	1916	7.5	0.730	1.033	999	1134

CFR10%	2154	2280	5.5	1.071	1.274	933	1032
CFR20%	1991	2123	6.2	0.896	1.183	958	1069
CFR30%	1828	1979	7.6	0.678	1.062	983	1120

Table 2: Dry and saturated thermo-physical properties for 120mm slump PRC mixes

	ρ_d	ρ_{sat}	n_{ap}	λ_{dry}	λ_{sat}	c_{dry}	c_{sat}
	kg/m^3	kg/m^3	%	W/(m K)	W/(m K)	J/(kg K)	J/(kg K)
Ref.	2296	2385	3.7	1.269	1.376	903	970
FR 10%	2162	2284	5.3	1.069	1.140	924	1020
FR20%	2039	2179	6.4	0.800	1.060	944	1060
FR30%	1878	2044	8.1	0.686	0.927	965	1112
CR10%	2091	2223	5.9	0.875	1.156	934	1041
CR20%	1944	2071	6.1	0.815	1.047	965	1075
CR30%	1754	1913	8.3	0.708	0.823	996	1146
CFR10%	2177	2238	5.4	1.100	1.083	929	1027
CFR20%	2016	2136	5.6	0.959	1.007	955	1056
CFR30%	1911	2031	5.9	0.848	0.996	980	1087

Table 3: Dry and saturated thermo-physical properties for 65mm slump PRC mixes

	ρ_d	ρ_{sat}	n_{ap}	λ_{dry}	λ_{sat}	c_{dry}	c_{sat}
	kg/m^3	kg/m^3	%	W/(m K)	W/(m K)	J/(kg K)	J/(kg K)
Ref.	2311	2390	3.3	1.358	1.448	901	961
FR 10%	2179	2292	4.9	1.074	1.349	921	1010
FR20%	2081	2217	6.1	0.922	1.186	942	1053
FR30%	1934	2100	7.9	0.814	0.986	963	1107
CR10%	2126	2248	5.4	1.092	1.230	932	1030
CR20%	1956	2113	7.4	1.010	1.054	963	1098
CR30%	1806	1955	7.6	0.790	1.027	994	1132
CFR10%	2157	2273	5.1	0.942	1.251	927	1020
CFR20%	2022	2147	5.8	0.832	1.11	952	1057
CFR30%	1827	1982	7.8	0.779	1.008	978	1120

Table 4: Dynamic thermal admittance properties for a 100mm thick external wall made using 180mm slump PRC mixes

	Y	ω	f	ϕ	F	ψ	U	κ	κ_{30}
	W/(m^2 K)	hr	-	hr	-	hr	W/(m^2 K)	kJ/(m^2 K)	kJ/(m^2 K)
Ref.	4.84	0.99	0.84	2.81	0.42	1.49	3.92	104	62
FR10%	4.71	1.01	0.85	2.75	0.44	1.43	3.82	98	59
FR20%	4.64	1.06	0.84	2.82	0.45	1.42	3.71	97	58
FR30%	4.43	1.14	0.84	2.88	0.48	1.38	3.46	93	56
CR10%	4.68	1.02	0.85	2.74	0.44	1.42	3.79	97	58
CR20%	4.53	1.07	0.85	2.74	0.46	1.37	3.64	92	55
CR30%	4.26	1.22	0.84	2.94	0.51	1.33	3.25	89	53
FCR10%	4.73	1.03	0.84	2.83	0.44	1.46	3.80	100	60
FCR20%	4.52	1.11	0.84	2.89	0.47	1.41	3.55	95	57
FCR30%	4.22	1.27	0.83	3.07	0.52	1.35	3.15	90	54

Table 5: Dynamic thermal admittance properties for a 100mm thick external wall made using 120mm slump PRC mixes

	Y	ω	f	ϕ	F	ψ	U	$\mathbf{K}$	κ_{30}
	W/(m^2 K)	hr	-	hr	-	hr	W/(m^2 K)	kJ/(m^2 K)	kJ/(m^2 K)
Ref.	4.90	0.95	0.85	2.74	0.41	1.49	4.02	104	62
FR10%	4.72	1.03	0.84	2.81	0.44	1.45	3.79	100	69
FR20%	4.44	1.18	0.83	3.04	0.48	1.42	3.39	96	58
FR30%	4.24	1.26	0.83	3.08	0.51	1.36	3.17	91	54
CR10%	4.53	1.13	0.83	2.97	0.47	1.43	3.50	98	59
CR20%	4.42	1.16	0.84	2.95	0.48	1.39	3.41	94	56
CR30%	4.22	1.23	0.84	2.95	0.51	1.33	3.21	87	52
FCR10%	4.76	1.01	0.84	2.81	0.44	1.46	3.83	101	61
FCR20%	4.59	1.08	0.84	2.83	0.46	1.41	3.65	96	58
FCR30%	4.45	1.14	0.84	2.91	0.48	1.39	3.47	94	56

Table 6: Dynamic thermal admittance properties for a 100mm thick external wall made using 65mm slump PRC mixes

	Y	ω	f	ϕ	F	ψ	U	κ	κ_{30}
	W/(m^2 K)	hr	-	hr	-	hr	W/(m^2 K)	kJ/(m^2 K)	kJ/(m^2 K)
Ref.	4.96	0.92	0.85	2.70	0.40	1.45	4.10	105	63
FR10%	4.74	1.03	0.84	2.84	0.44	1.46	3.80	101	61
FR20%	4.59	1.10	0.83	2.94	0.46	1.44	3.59	99	59
FR30%	4.42	1.16	0.84	2.95	0.48	1.39	3.41	94	56
CR10%	4.73	1.02	0.84	2.79	0.44	1.45	3.82	100	60
CR20%	4.71	1.04	0.85	2.74	0.45	1.40	3.72	95	57
CR30%	4.35	1.17	0.84	2.89	0.49	1.35	3.37	90	54
FCR10%	4.63	1.10	0.83	2.97	0.46	1.46	3.62	101	60
FCR20%	4.48	1.16	0.83	3.01	0.48	1.42	3.45	97	58
FCR30%	4.33	1.18	0.84	2.90	0.49	1.35	3.35	90	54

Figure 1: Dynamic thermal response of 180mm slump mix

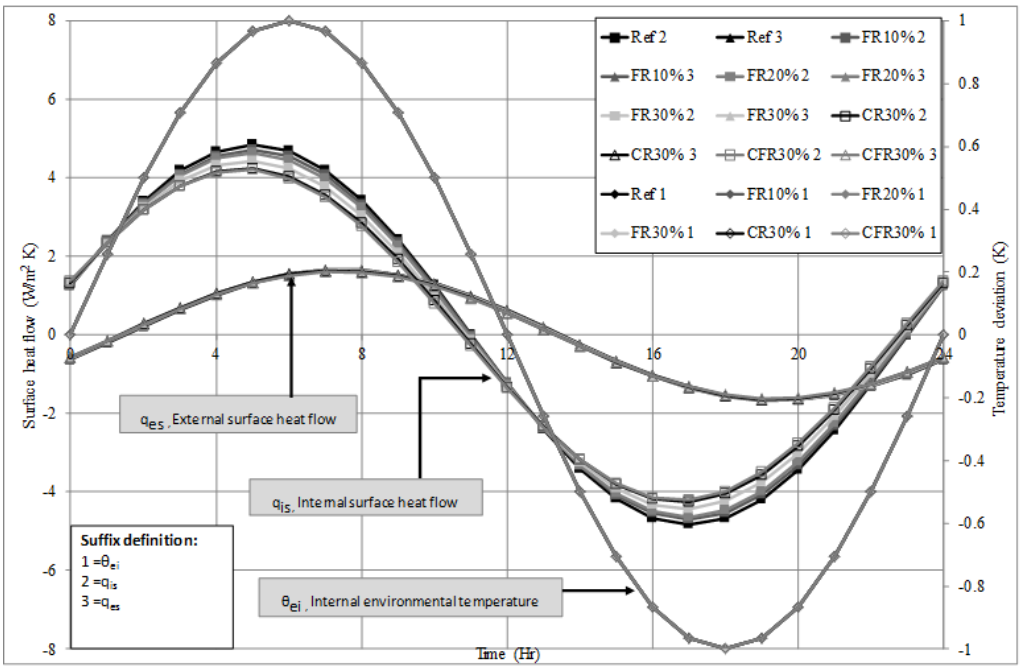

Figure 2: Dynamic thermal response of 120mm slump mix

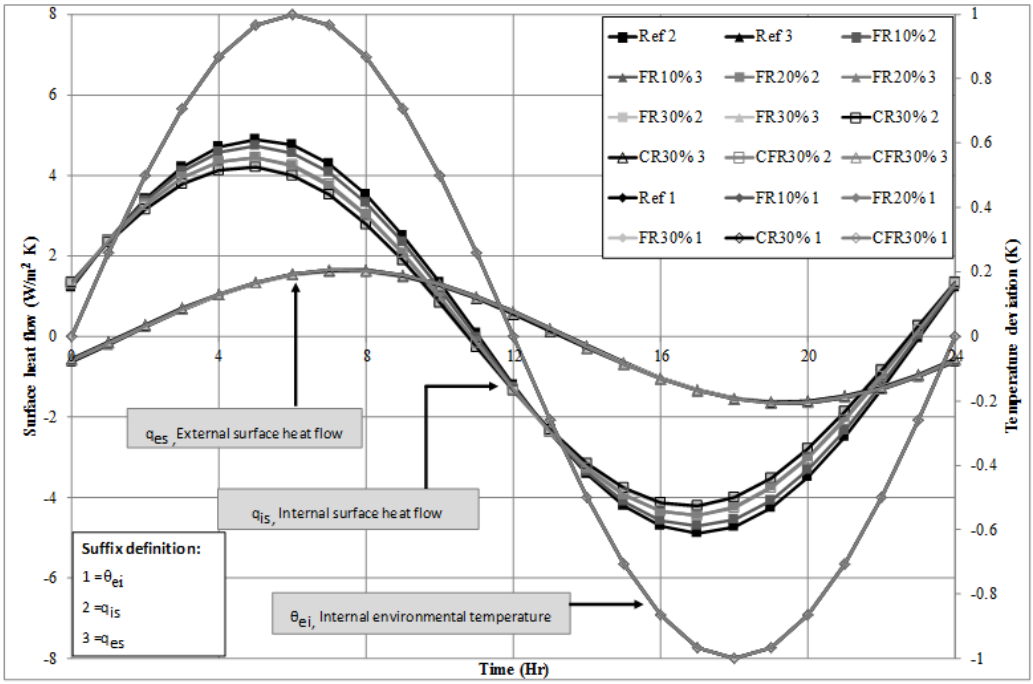

Figure 3: Dynamic thermal response of 65mm slump mix